RSC Advances

PAPER

View Article Online
View Journal | View Issue

Cite this: *RSC Adv.*, 2023, **13**, 27525

Design, synthesis, molecular docking and DFT studies on novel melatonin and isatin based azole derivatives†

Keshav Kumar Saini,[ab] Ravindra Kumar Upadhyay,[ac] Ravi Kant,[d] Arpita Vajpayee,[e] Kalpana Jain,[f] Amit Kumar,[b] Lalita S. Kumar[g] and Rakesh Kumar*[a]

In order to address the pressing demand for newer broad-spectrum antifungal medicines with enhanced activity, computer modelling was utilised to rationally develop newer antifungal azole-based drugs. Based on the drug and active sites of the *Lanosterol* 14 alpha-Demethylases (LAD) of the prominent fungal pathogen *Candida albicans* interaction, Novel triazole-linked melatonin and isatin derivatives **7a–d** and **8a–d** were synthesised using bioisosterism. Besides the experimental synthesis and subsequent characterization, the present study focused on obtaining optimised geometries, frequency calculations, and TD-DFT studies of the synthesised molecules. We also performed molecular docking studies to explore the inhibitory ability of the synthesised compounds against the active sites of the *Lanosterol* 14 alpha-Demethylases (LAD) of the prominent fungal pathogen *Candida albicans*. The binding interactions resulted in positive findings, demonstrating the involvement of the synthesised compounds in the suppression of fungal growth. Comparative analysis of the binding potential of the synthesised molecules and commercially available drug fluconazole revealed a remarkable note: the docking scores for the designed drugs **7b**, **7c**, and **8c** are much greater than those of the fluconazole molecule. The *in silico* study of the designed series of drug molecules serves as an important guideline for further exploration in the quest for potent antifungal agents.

Received 14th August 2023
Accepted 1st September 2023

DOI: 10.1039/d3ra05531k

rsc.li/rsc-advances

Introduction

Heterocycles are an immensely important class of organic compounds, accounting for more than half of all documented organic molecules. They serve as an important core moiety in a wide range of natural products, including haemoglobin, biomolecules, RNA, DNA, proteins, vitamins, and biologically active compounds.[1] Heterocyclic scaffolds are important synthetic precursors for the synthesis of a variety of biologically active compounds. According to recent surveys, an enormous number of molecules are under investigation by researchers, including nitrogen-containing heterocycles such as indoles, pyrimidyl, pyrazolyl, thiazolyl, and pyridyl indoles, for their applications in the field of pharmacological and therapeutic effects.[2–4] Naturally occurring melatonin belongs to the privileged class of indoleamine, which is synthesised and discovered in a variety of species, including bacteria and eukaryotes.[5] Melatonin is a pineal gland hormone produced by serotonin that governs the cycle of sleep and wakefulness, the circadian rhythm, cycles of menstruation, ageing, immunity, and antioxidants in the body, among other things. Melatonin production and release are more intense at night, whereas light exposure suppresses them.[6] Previous research has documented that melatonin has a wide range of physiological effects, including antioxidant,[7,8] cardiovascular,[9,10] anti-inflammatory,[11,12] neuroprotective,[13,14] stroke protective,[15] pain modulatory,[16] antitumor,[17] antibacterial,[18,19] liver injury protective properties,[20] retinal,[21] as well as effects on offspring metabolism,[22] *etc.* 1*H*-indole-2,3-dione, which is commonly referred to as Isatin or indenedione, is a versatile moiety with a broad range of biological activity. Isatin is the precursor for a number of derivatives that possess a broad range of potential biological and pharmaceutical properties[23] such as anticancer properties in various types of cancers,[24–26] antibiotics,[27] anxiogenic,[28] antibacterial,[29] antidiabetic,[30] anticonvulsant,[31] sedative,[32]

[a]*Department of Chemistry, University of Delhi, Delhi 110007, India. E-mail: rakeshkp@email.com*

[b]*Department of Chemistry, Dyal Singh College, University of Delhi, Lodhi Road, New Delhi 110003, India*

[c]*Department of Chemistry, Sri Venkateswara College, University of Delhi, New Delhi 110021, India*

[d]*Department of Chemistry, Government Post Graduate College, G.B. Nagar, Noida, UP 201301, India*

[e]*Department of Physics, Dyal Singh College, University of Delhi, Lodhi Road, New Delhi 110003, India*

[f]*Department of Physics, D. J. College, Baraut, UP 250611, India*

[g]*Chemistry Discipline, School of Sciences, Indira Gandhi National Open University, New Delhi 110068, India*

† Electronic supplementary information (ESI) available. See DOI: https://doi.org/10.1039/d3ra05531k

carboxylesterases,[33] antidepressants,[34] antifungals,[35] antimicrobial[36] *etc.* Triazoles, namely 1,2,3-triazole and 1,2,4-triazole, are among the most significant groups of nitrogen-containing heterocycles. Triazole may increase solubility and binding to bimolecular targets *via* a variety of non-covalent interactions.[37] Triazoles are known to possess a wide number of biological activities, such as antimicrobial, antihistaminic, analgesic, anti-inflammatory, antimycotic, anticancer, antiprotozoal, insecticidal, antimalarial, anticonvulsant, antimycobacterial, and anti-ulcer activity.[38,39] The 14α-demethylase enzyme (CYP51), also known as *lanosterol*, is essential for the biosynthesis of ergosterol. By inhibiting ergosterol production, fungal growth is inhibited.[40]

The incorporation of two or more pharmacophores into a single hybrid molecule *via* triazole link delivers an appealing approach to facilitating the development of newer drugs with the capacity to overcome cross-resistance and enhance potency in comparison to the individual moiety. Based on the aforementioned details and our keen interest in discovering newer, more potent antifungal agents to overcome drug resistance, we are reporting a simple technique for the synthesis of novel *N*-(2-(1-((1-(2-(2,3-dioxoindolin-1-yl)ethyl)-1*H*-1,2,3-triazol-5-yl) methyl)-5-methoxy-1*H*-indol-3-yl)ethyl)acetamide and its derivatives *via* alkyne-azide cycloaddition catalysed by Cu(I) (CuAAC) reaction. In the present investigation, we also reported the molecular docking study of all synthesised molecules in order to forecast probable binding modalities with *Lanosterol* 14 alpha-Demethylases (LAD) of prominent fungal pathogens *Candida albicans* to block sites responsible for ergosterol biosynthesis. The outcomes seem to strongly indicate that the synthesised compounds hold promise as potential antifungal drug molecules, thus, the outcome of the present study serve as important guidelines for further scientific exploration of these potential candidates for use in *in vitro* and *in vivo* studies for the development of efficient antifungal agents.

Design strategy

Furthermore, numerous clinically approved and under-trial drugs with robust antifungal characteristics are based on melatonin, isatin, and 1,2,3-triazole rings, making the melatonin, isatin, and 1,2,3-triazole core a fascinating and understudied pharmacophore. In continuation of our keen interest in the designing of single drug with multiple targets, we have synthesised new hybrids by inclusion of melatonin, isatin, and triazole scaffolds into a single target molecule (Fig. 1).

Result discussion

Methods and materials

All the reagents required for the current study were analytical reagent grade and were used as such without further purification. All the reagents and materials were procured from Sigma Aldrich, Merk, and Spectrochem from commercial suppliers. All the solvents were purchased from Finar Ltd. All the reactions were monitored with thin layer chromatography silica gel plates (TLC) Kieselgel 60 F_{254} (Merk) using ethyl acetate/petrol or methanol/chloroform as mobile phases and visualised in UV light. The purification of all synthesised molecules was carried out using silica gel 100–200 Mesh (Qualikems). The melting points of all synthesised molecules were determined by the electrothermal melting point apparatus Buchi instrument (M-560) and were uncorrected. Infrared spectra were recorded using KBr pellets on a SHIMADZU FT-IR affinity spectrophotometer, and the recordings are expressed as υ_{max} cm^{-1}. The formation of the synthesised molecule was confirmed by ^1H

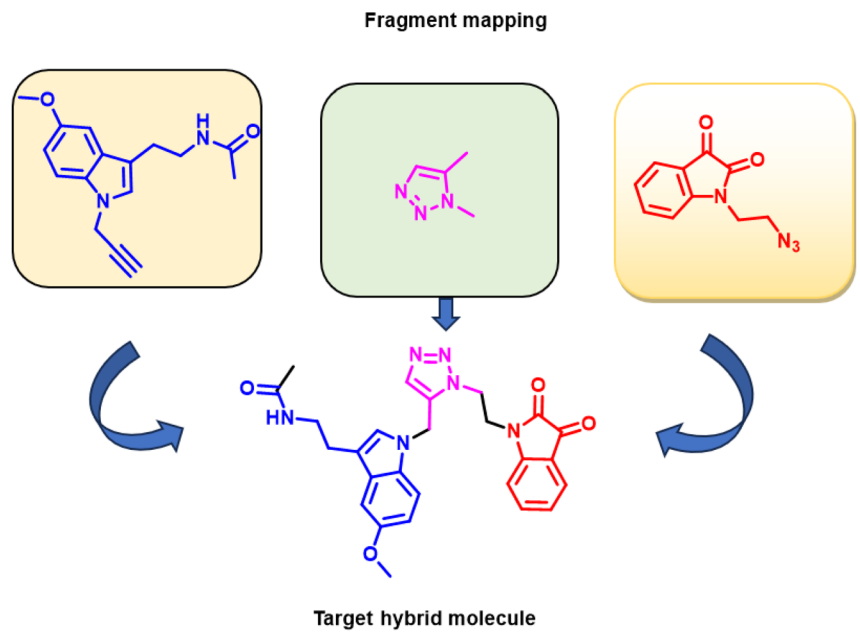

Fig. 1 Melatonin, triazole, and isatin-based antifungal agents, mapped to the designed target compound.

NMR and ^{13}C NMR on a JEOL, ECX-400P spectrometer USA at 400 MHz and 100 MHz using tetramethylsilane (TMS) as an internal reference standard. The chemical shift (δ), coupling constant, and absorption frequency for the NMR spectra were reported as parts per million, J (Hz), and ν (cm^{-1}), respectively in dimethyl sulfoxide (DMSO-d$_6$) as the solvent. The spectral data uses the notation s, d, t, q, dd, and m for singlet, doublet, triplet, quartet, doublet of doublet, and multiplate, respectively. All mass spectrometry readings for all synthesised compounds were taken using a 6530 Accurate-Mass Q-TOF LC/MS instrument.

Method of preparations

The synthesised target molecules **7a–d** and **8a–d** in the present work include three fundamental structural elements: (i) *N*-substituted melatonin; (ii) a substituted 1,2,3-triazole moiety; and (iii) a substituted isatin moiety. The procedure for the synthesis of triazole-linked melatonin isatine derivatives was accomplished in four steps, beginning with the reaction of melatonin (**1**) with one equivalent of propargyl bromide and NaH in DMF at RT to get *N*-(2-(5-methoxy-1-(prop-2-yn-1-yl)-1*H*-indol-3-yl)ethyl) acetamide (**2**) in 91% yield (Scheme 1). Following that, a variety of nonpolar, polar aprotic, and polar protic solvents (entries 1–12) were tested with K_2CO_3 and NaH bases, and the experimental findings suggested that reaction with NaH in DMF (entry 10) was the most appropriate choice for the current chemical reaction under investigation (Table 1).

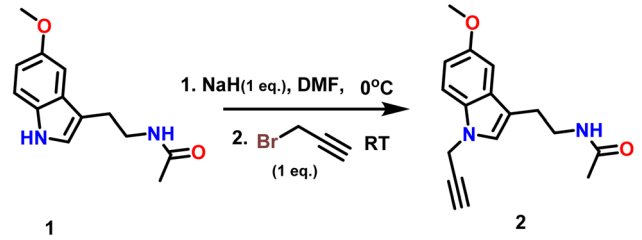

Scheme 1 Synthesis of propargylated derivative of melatonin **1** 1(1 eq), NaH (1 eq).

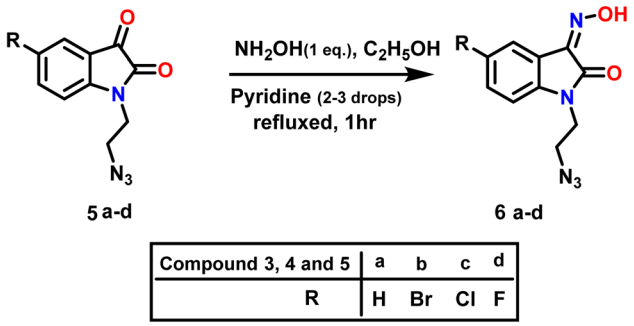

Scheme 3 Synthesis of *N*-alkylazido-hydroxyiminoisatins derivatives (6a–d).

Table 1 Standardisation of reaction conditions for propargylation of melatonin

Entry	Solvent	Base	Number of equivalents (base)	Temp (°C)	Time (h)	Yield (%)
1	Toluene	K_2CO_3	1	RT	8	No reaction
2	Toluene	NaH	1	RT	8	No reaction
3	Xylene	K_2CO_3	1	RT	8	No reaction
4	Xylene	NaH	1	RT	8	No reaction
5	THF	K_2CO_3	1	RT	8	23
6	THF	NaH	1	RT	8	25
7	ACN	K_2CO_3	1	RT	6	36
8	ACN	NaH	1	RT	6	38
9	DMF	K_2CO_3	1	RT	3.0	85
10	**DMF**	**NaH**	**1**	**RT**	**1.5**	**91**
11	*t*-Butanol	K_2CO_3	1	RT	5	42
12	*t*-Butanol	NaH	1	RT	5	42

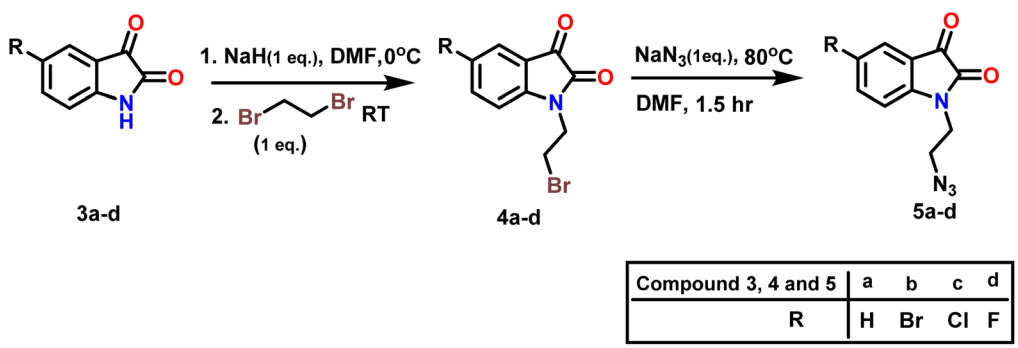

Scheme 2 Synthesis of 2-azidoethyl-Isatins derivatives (5a–d).

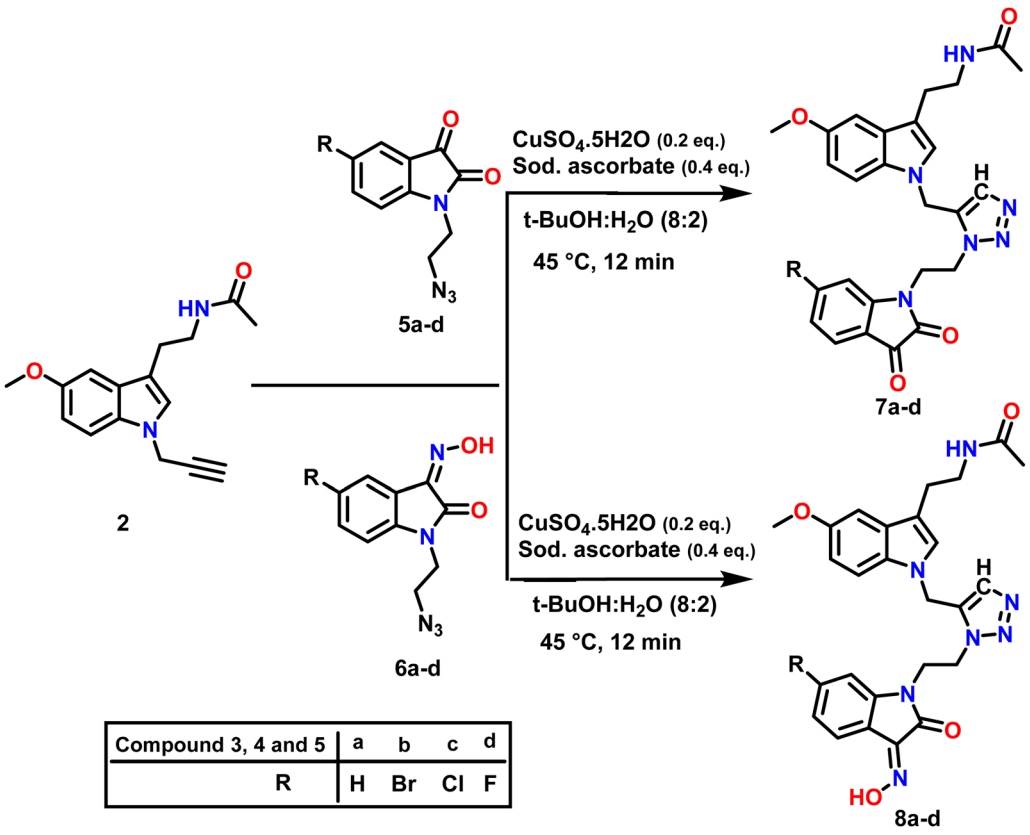

Scheme 4 Synthesis of target compound 7a–d and 8a–d using click reaction.

In step 2 azide derivatives of isatin (**5a–d**)were synthesised according to the reported methods.[41,42] Alkylation of substituted isatin (**3a–d**) with 1,2-dibromoethane yielded **4a–d** in presence of NaH and DMF Scheme 2. 3 and 4. The resulting *N*-alkylbromoisatins (**4a–d**) were subsequently treated with sodium azide in DMF at 80 °C to give the corresponding *N*-alkylazidoisatins (**5a–d**).

The precursor, **5a–d** were further refluxed with hydroxyl amine in pyridine and ethanol for 1 h to give a *N*-alkylazidohydxoxyiminoisatins[43] (**6a–d**).

In an attempt to adopt an environmentally friendly green method for the synthesis of the target compound **7a–d** and **8a–d**. We used Cu(I) catalysed click reaction by reported methods[44,45] (Table 2). But these reactions have been going on for a long time at high temperatures, and the yield in response to them is also discouraging (Table 2 entries no. 1, 4, and 5). Therefore, target compounds were prepared by Cu(I)-catalyzed click reactions *via* 1,3-dipolar cycloaddition in t-BuOH-H_2O (entry 3: Table 2) to get better yield. Thus, *N*-propargylated melatonin (**2**) was allowed to react with isatin and substitute isatin azides **5a–d** and **6a–d** in t-BuOH-H_2O (8 : 2) (1 : 1) using $CuSO_4$ and sodium ascorbate as catalysts at 45 °C for 12–18 minutes to afford corresponding 1,4-disubstituted 1,2,3-triazoles (**7a–d**, **8a–d**) in excellent yield (Table 3).

The Structure of synthesised compounds were characterised using ^{1}H NMR, ^{13}C NMR, FTIR and HRMS analytical techniques. In the ^{1}H NMR of compound **7b**, a singlet was observed at δ 1.8 ppm for 3 protons of the CH_3 group attached to the amide group of melatonin. A singlet for 3 protons of methyl of the methoxy group attached to the aromatic ring of the melatonin core was observed at δ 3.76 ppm. A characteristic triplet was observed at δ 7.96 ppm for 1 proton, corresponding to the NH of the amide group of melatonin. A singlet appeared at δ 8.04 ppm for one proton for the triazole hydrogen. The ^{13}C

Table 2 Standardisation of reaction conditions for the Cu(I)-catalyzed alkyne-azide cycloaddition (CuAAC) reaction

S No.	Catalyst	Solvent	Reaction condition	Yield (%)
1	$CuSO_4$/Sod ascorbate	Water	120 °C 24 h	33
2	$CuSO_4$/Sod ascorbate	DMF + H_2O (1 : 1)	60 °C 15 min	86
3	**$CuSO_4$/Sod ascorbate**	***t*-BuOH/H_2O (8 : 2)**	**45 °C 12 min**	**90**
4	$CuSO_4$/Sod ascorbate	Ethanol	60 °C	No reaction
5	$CuSO_4$/Sod ascorbate	Ethanol/H_2O	60 °C	No reaction

Table 3 Structures of the synthesised compounds **7a–d** and **8a–d**

S No.	Compound no.	Structure	Melting point (°C)	Yield (%)
1	**7a**	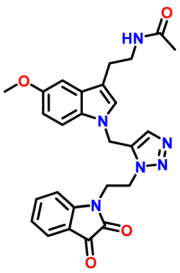	141–143	87
2	**7b**	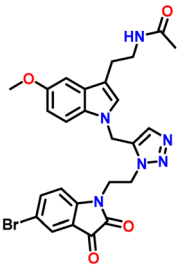	133–135	86
3	**7c**	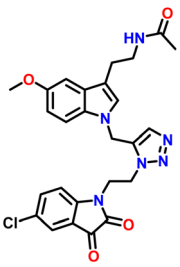	138–140	88
4	**7d**	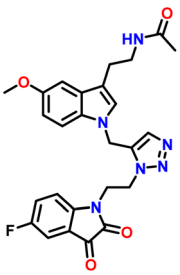	131–133	85
5	**8a**	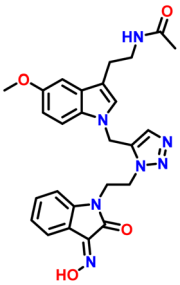	182–184	85
6	**8b**	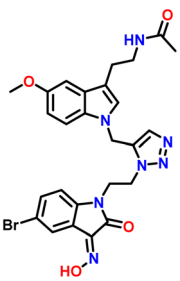	181–183	84

Table 3 (*Contd.*)

S No.	Compound no.	Structure	Melting point (°C)	Yield (%)
7	**8c**	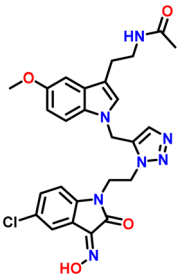	185–187	84
8	**8d**	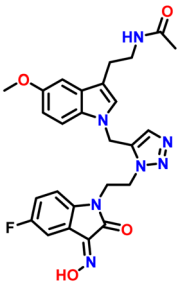	180–182	84

NMR spectrum of compound **7b** showed a peak at δ 182.20 ppm, which was assigned to the C=O (keto) carbon of the five-membered ring of isatin. The peak at δ 131.61 ppm corresponds to the carbon of the triazole ring. The peaks at δ 126.97 ppm were assigned to the carbon of the five-membered ring of melatonin.

In the ^{1}H NMR of compound **8c**, a singlet was observed at δ 1.80 ppm for 3 protons of the CH_3 group attached to the amide group of melatonin. A singlet for 3 protons of methyl of the methoxy group attached to the aromatic ring of the melatonin core was observed at δ 3.76 ppm. A characteristic triplet was observed at δ 7.93 ppm for 1 proton, corresponding to the NH of the amide group of melatonin. A singlet appeared as a singlet at δ 8.00 ppm for the triazole hydrogen. A singlet observed at δ 8.00 ppm, corresponding to the hydrogen of the hydroxy group of isatinoximes. The ^{13}C NMR spectrum of compound **8c** showed a peak at δ 163.16 ppm, which was assigned to the C=N carbon of the five-membered ring of isatin. The peak that appeared at δ 131.61 ppm corresponds to the carbon of the triazole ring. The peaks that appeared at δ 126.56 ppm were assigned to the carbon of the five-membered ring of melatonin.

Computational study

DFT studies. The molecular interaction study is being based upon obtaining structural parameters of optimized geometry of the designed series of molecules as a prior exercise to the molecular docking. The basis of this study is Density Functional Theory (DFT), using which the optimization of the ground state molecular geometry of the designed molecules has been performed using 6-311G** dp basis set at B3LYP level by employing

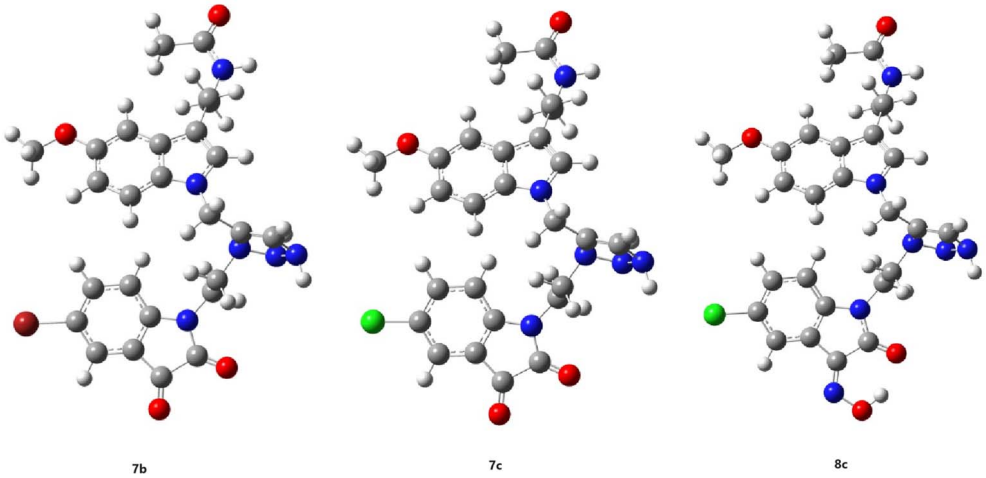

Fig. 2 Optimised geometrical structures of the designed molecules; **7b**, **7c** and **8c**.

Table 4 The interaction analysis of the *Lanosterol* 14 alpha-Demethylases enzyme on the basis of molecular docking studies with the triazole linked melatonin-isatin derivatives

S No.	Drug name (ligand)	Binding energy (kcal mol^{-1})	Hydrogen bond interaction	Hydrostatic interaction with amino acids
1	**6**	−7.3	—	Gly 65(A), Leu 87(A), Leu 88(A), Lys 90(A), Tyr A: 122, Pro 230(A), Phe 233(A), Ile 231(A), His 377(A), Phe 380(A), Ser 507(A), Met 508(A)
2	**7a**	−10.1	His 377(A) 3.25 Å, Met 508(A) 2.91 Å	Gly 65(A), Leu 87(A), Leu 88(A), Tyr 118(A), Thr 122(A), Phe 228(A), Pro 230(A), Phe 233(A), Leu 376(A), Ser 378(A), Phe 380 (A), Tyr 505(A), Ser 506(A), Val 509(A)
3	**7b**	−11.1	Ser 378(A) 2.65 Å	Leu 87(A), Tyr 118(A), Thr 122(A), Tyr 132(A), Pro 230(A), Phe 233(A), Gly 307(A), His 310(A), Thr 311(A), Leu 376(A), Ile 379(A), Phe 380(A), Ser 507(A), Met 508(A), Val 509(A)
4	**7c**	−11.0	Ser 378(A) 3.08 Å, Met 508(A) 2.92 Å	Leu 87(A), Tyr 118(A), Leu 121(A), Thr 122(A), Phe 126(A), Tyr 132(A), Phe 228(A), Pro 230(A), Phe 233(A), Gly 307(A), Thr 311(A), Leu 376(A), His 377(A), Phe 380(A), Ser 507(A)
5	**7d**	−10	Ser 378(A) 3.18 Å, Met 508(A) 3.09 Å	Gly 65(A), Leu 87(A), Leu 88(A), Tyr 118(A), Thr 122(A), Phe 228(A), Pro 230(A), Phe 233(A), Leu 376(A), His 377(A), Phe 380(A), Tyr 505(A), Ser 506(A), Val 509(A)
6	**8a**	−9.1	Asp 225(A) 2.87 Å, Met 189(A) 3.06 Å, His 310(A) 2.88 Å	Glu 194(A), Ile 197(A), Pro 193(A), Phe 213(A), Ala 218(A), Tyr 221(A), Ser 222(A), Phe 228(A), Gln 309(A), Ser 507(A), Met 508 (A), Val 509(A), Leu 511(A)

Table 4 (*Contd.*)

S No.	Drug name (ligand)	Binding energy (kcal mol^{-1})	Hydrogen bond interaction	Hydrostatic interaction with amino acids
7	**8b**	−8.9	Asp 225(A) 2.70 Å	Glu 194(A), Met 189(A), Pro 193(A), Ile 197(A), Phe 198(A), Ala 218(A), Tyr 221(A), Ser 222(A), Phe 228(A), His 310(A), Gln 309(A), Ala 313(A), Ser 314(A), Ser 507(A), Met 508 (A), Leu 511(A)
8	**8c**	−11.6	His 377(A) 2.94 Å, Ser 378(A) 2.92 Å	Leu 87(A), Tyr 118(A), Tyr 132(A), Phe 228(A), Pro 230(A), Phe 233(A), 307(A), Thr 311(A), Leu 376(A), Phe 380(A), Tyr 505(A), Ser 507(A), Met 508(A)
9	**8d**	−9.2	Asp 225(A) 2.80 Å	Met 189(A), Pro 193(A), Glu 194(A), Ile 197(A), Phe 198(A), Phe 213(A), Ala 218(A), Tyr 221(A), Ser 222(A), Phe 228(A), Gln 309(A), His 310 (A), Ala 313(A), Ser 314(A), Ser 507(A), Met 508 (A), Val 509(A), Leu 511(A)
10	Fluconazole	−8.2	—	Tyr 118(A), Leu 121(A), Thr 122(A), Ile 131(A), Tyr 132(A), Hem O(B), Phe 228(A), Gly 303(A), Gly 307(A), Leu 376(A), Met 508(A), Val 509(A)

Gaussian 09 software. The frequency calculations on the optimized geometry have also been analysed for presence of any negative frequency. The absence of any negative frequency bears a clear indication that the optimized geometry corresponds to a stable structure (Fig. 2) at local minima. The structural parameters of the optimized geometry in respect of each of the studied molecule is shown in as ESI.† The electronic structure calculations on optimised geometry have been followed by time dependent DFT (TD-DFT) study aimed at obtaining the theoretically studied electronic spectra of the designed molecules. A comparison of the theoretically studied vibrational frequencies of the designed molecules with the experimentally obtained FT-IR spectra clearly reveals a strong concordance which gives us confidence in our study to proceed further and pursue molecular docking.

Molecular docking. Molecular docking provides a theoretical direction for visual representation of the binding characteristics of ligand molecule to the protein under study and serve as guidelines for further exploration and substantiation of experimental data. On the basis of the optimised structures of the designed series of molecules, the molecular docking study has been carried out for each of the studied molecule using AutoDoc Vina software package. The main objective of the molecular docking study lies at the evaluation of binding potential along with molecular interaction of the designed molecule with varied amino acid residues of the membrane protein; *Lanosterol* 14 alpha-Demethylases (LAD) of prominent fungal pathogens *Candida albicans*. The three-dimensional (3D) crystal structures of *Lanosterol* 14 alpha-Demethylases (PDB ID: 5v5z) was obtained from protein databank. The molecular docking was performed for the important binding site of the protein by setting the grid size to 40, 40, 40 along the cartesian axis *x*, y, *z* keeping the grid spacing to 0.375 Å. The grid centre has been set to −45.704, 16.276, −14.957, 25.341 for the studied binding site. The visualization of protein-ligand complex was performed using PYMOL software package. The docking score for the studied molecules *i.e.*, **6**, **7a–d** and **8a–d** is shown in Table 4. The magnitude of binding energy follows the order **8c** > **7b** > **7c** > **7a** > **7d** > **8d** > **8a** > **8b** > **6** for the studied molecules with highest value of −11.6 kcal mol^{-1} and the lowest being −7.3 kcal mol^{-1} (Fig. 5). Among the various studied molecules, the best docked conformations of the LAD-**8c**, LAD-**7b** and LAD-**7c** complex, with the highest docking score, in the studied binding site of the protein are shown in Fig. 3. All the docked conformers were further analysed by the Ligplot analysis tool for a better insight into the molecular interactions of the ligands with the amino acid residues on the surface of LAD and the results of molecular interactions are shown in Fig. 4. It is evident from Fig. 4 that the ligand molecules exhibit both hydrophobic interactions as well as hydrogen bonding with the amino acid residues on the

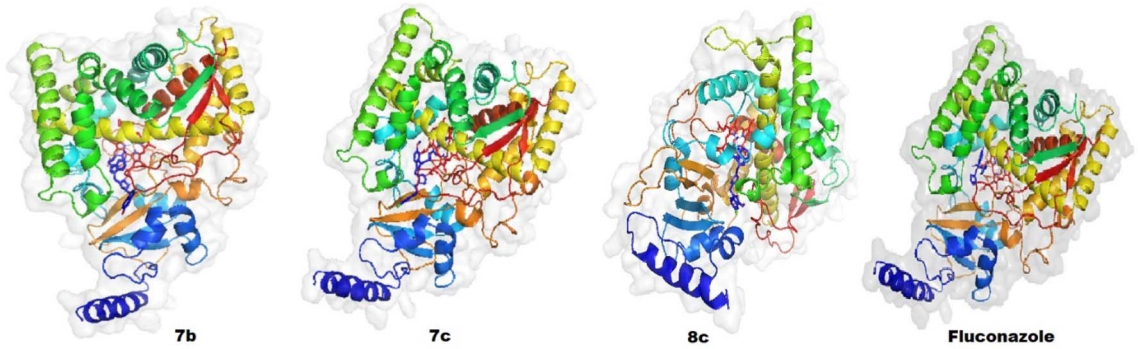

Fig. 3 The best docked molecules **7b**, **7c**, and **8c** to *Lanosterol* 14 alpha-Demethylases protein with the highest docking score of −11.1 kcal mol^{-1} (**7b**), −11.0 kcal mol^{-1} (**7c**) and −11.6 kcal mol^{-1} (**8c**) as compared with standard drug fluconazole (−8.2 kcal mol^{-1}).

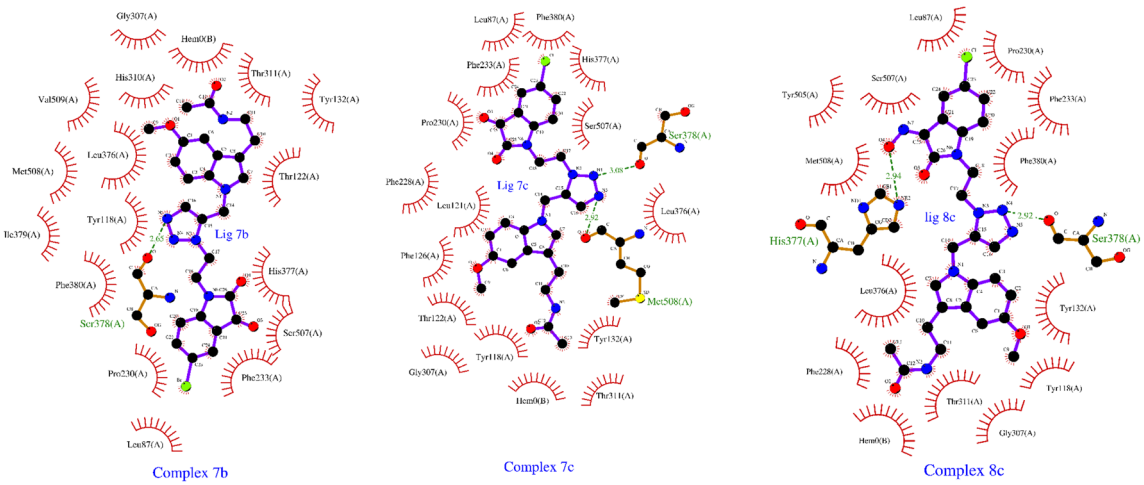

Fig. 4 Detailed depiction of molecular interaction of the ligand molecules (**7b**, **7c**, and **8c**) having highest binding energy, with various amino acid residue in the binding pocket of the protein *Lanosterol* 14 alpha-Demethylases of prominent fungal pathogens *Candida albicans*.

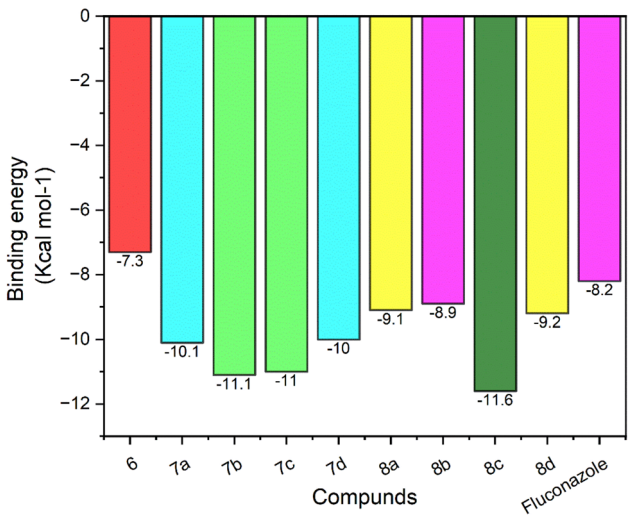

Fig. 5 The docking score for the synthesised molecules *i.e.*, **6**, **7a–d**, **8a–d** and commercially available fluconazole drug with reference to their binding energy.

surface of LAD protein in the binding site. As a striking feature, it is interesting to note that the oxime substituted isatin derevatives (molecules **8a** and **8c**) exhibit twin H-bond binding interaction using both the triazole and isatin moieties, present within the molecular framework, with the amino acid residues on the surface of the protein, however, the unsubstituted isatin derivatives (molecules **7a–7d**) binds at the triazole group site only. The highest docking score of −11.6 kcal mol^{-1} has been obtained for molecule **8c**. These results reveal the importance of substitution of the isatine moiety for enhanced binding interaction of the drug molecules. These trends on exhibition of strong binding with the protein by the molecules having substitution of isatin moiety in the molecular framework have also been exhibited by Singh *et al.* in their study on isatin-benzotriazole hybrids.[46] Further, it is important to note that substituted derivatives *i.e.*, molecules **8a–d**, exhibit hydrogen bonding through isatin moiety with His 377(A), Asp 225(A) amino acid residues, however, H- bond formation involving triazole moiety occurs with Ser 378(A). More importantly, Ser 378(A) is also the preferred site for H-bond formation trough triazole moiety in unsubstituted molecules **7a–d** also. Ligplot

results further show a strong hydrophobic interaction of the ligand with the amino acids as described in Table 4. As an interesting common feature, the molecules with highest docking score *i.e.*, **7b**, **7c** and **8c** exhibited notably strong hydrophobic interaction with heme moiety present in the active site of the protein, thus one can draw significance of this interaction in enhanced binding interaction of the molecules with CYP51 protein for exhibiting enhanced antifungal activity of the drug molecules. The significance of this kind of interaction with heme moiety present in the active site of CYP51 has also been highlighted by Shaikh *et al.*[47] in their molecular docking study of 1,2,3,-Triazole tethered acetophenone ligand molecules. Moreover, hydrophobic interactions of the best docked molecules with the amino acid residue Leu 87(A), Tyr 118(A), Pro 230(A), Phe 228(A), Phe 233(A), Thr 311(A), Leu 376(A), Phe 380(A), and Ser 507(A) marks a common feature in the ligplot results analysis of the molecular interaction of the ligand with the amino acid residue on the surface of the protein.

Conclusion

In conclusion, a targeted library of structurally varied substituted 1,2,3-triazoles comprising melatonin and isatin cores was mapped and effectively synthesised by Cu(I)-sodium ascorbate catalysed click reaction. A broad range of 1,2,3-triazoles has been synthesised in excellent yield and characterised by ^{1}H NMR and ^{13}C NMR, FT-IR, and HRMS analytical techniques. Following the synthesis of the targeted hybrid compounds, molecular docking assesses with the *Lanosterol* 14 alpha-Demethylases have been performed to validate the binding ability of synthesised compounds to inhibit *Lanosterol* 14 alpha-Demethylases active sites. Among all docked molecules, the oxime substituted isatin derivative molecules **8c** followed by **7b** and **7c** compounds significantly block the active site of targeted enzyme. The concept of combining physiologically active moieties in a single hybrid molecule prove to be a workable strategy to design novel strategic drug molecules for facilitating for design and synthesis of potential antifungal therapeutic candidates. These results are important guideline for further exploration and testing for potent antifungal agents.

Conflicts of interest

The authors affirm that there are no conflicts of interest in this article's content.

Acknowledgements

KKS is grateful to the Institutions of Eminence (IoE) for providing funds to carry out the present research work. KKS also grateful to the University of Delhi's USICU (University Science Instrumentation Centre), IIT Delhi for providing the required instrumentation facilities and access to the Supercomputing Facility for Bioinformatics and Computational Biology Center, IIT, Delhi for carrying out electronic structure calculations on the studied molecules. Authors also gratefully acknowledge CSIR for financial support for this work.

References

1 B. Eftekhari-Sis, M. Zirak and A. Akbari, *Chem. Rev.*, 2013, **113**, 2958–3043.
2 H. Mizoguchi, H. Oikawa and H. Oguri, *Nat. Chem.*, 2014, **6**, 57–64.
3 H. Liu and A. Dömling, *J. Org. Chem.*, 2009, **74**, 6895–6898.
4 A. Kumari and R. K. Singh, *Bioorg. Chem.*, 2019, **89**, 103021.
5 N. Ferlazzo, G. Andolina, A. Cannata, M. G. Costanzo, V. Rizzo, M. Currò, R. Ientile and D. Caccamo, *Antioxidants*, 2020, **9**, 1–29.
6 D. Acuña-Castroviejo, G. Escames, C. Venegas, M. E. Díaz-Casado, E. Lima-Cabello, L. C. López, S. Rosales-Corral, D. X. Tan and R. J. Reiter, *Cell. Mol. Life Sci.*, 2014, **71**, 2997–3025.
7 M. S. Estevão, L. C. Carvalho, D. Ribeiro, D. Couto, M. Freitas, A. Gomes, L. M. Ferreira, E. Fernandes and M. M. B. Marques, *Eur. J. Med. Chem.*, 2010, **45**, 4869–4878.
8 Z. A. Velkov, Y. Z. Velkov, B. T. Galunska, D. N. Paskalev and A. V. Tadjer, *Eur. J. Med. Chem.*, 2009, **44**, 2834–2839.
9 A. Lochner, E. Marais and B. Huisamen, *J. Pineal Res.*, 2018, **65**, 1–22.
10 H. Sun, A. M. Gusdon and S. Qu, *Curr. Opin. Lipidol.*, 2016, **27**, 408–413.
11 X. Chen, C. Sun, P. Laborda, Y. He, Y. Zhao, C. Li and F. Liu, *Plant Pathol.*, 2019, **68**, 288–296.
12 X. Chen, C. Sun, P. Laborda, Y. Zhao, I. Palmer, Z. Q. Fu, J. Qiu and F. Liu, *Front. Microbiol.*, 2018, **9**, 1–14.
13 D. Alonso-Alconada, A. Álvarez, O. Arteaga, A. Martínez-Ibargüen and E. Hilario, *Int. J. Mol. Sci.*, 2013, **14**, 9379–9395.
14 B. S. Alghamdi, *J. Neurosci. Res.*, 2018, **96**, 1136–1149.
15 H. W. Lin and E. J. Lee, *Neuropsychiatr. Dis. Treat.*, 2009, **5**, 157–162.
16 S. A. zeved de Zanette, R. Vercelino, G. Laste, J. R. ipol. Rozisky, A. Schwertner, C. B. uzzatt. Machado, F. Xavier, I. C. ristin, C. de Souza, A. Deitos, I. L. S. Torres and W. Caumo, *BMC Pharmacol. Toxicol.*, 2014, **15**, 40.
17 G. Di Bella, F. Mascia, L. Gualano and L. Di Bella, *Int. J. Mol. Sci.*, 2013, **14**, 2410–2430.
18 L. Xu, W. Zhang, M. Kwak, L. J. Zhang, P. C. W. Lee and J. O. Jin, *Front. Immunol.*, 2019, **10**, 1–11.
19 F. He, X. Wu, Q. Zhang, Y. Li, Y. Ye, P. Li, S. Chen, Y. Peng, R. Hardeland and Y. Xia, *Front. Immunol.*, 2021, **12**, 1–15.
20 F. Ye, J. He, X. Wu, J. Xie, H. Chen, X. Tang, Z. Lai, R. Huang and J. Huang, *Biomed. Pharmacother.*, 2019, **117**, 109141.
21 G. Tosini, K. Baba, C. K. Hwang and P. M. Iuvone, *Exp. Eye Res.*, 2012, **103**, 82–89.
22 D. S. Ferreira, F. G. Amaral, C. C. Mesquita, A. P. L. Barbosa, C. Lellis-Santos, A. O. Turati, L. R. Santos, C. S. Sollon, P. R. Gomes, J. A. Faria, J. Cipolla-Neto, S. Bordin and G. F. Anhê, *PLoS One*, 2012, **7**(6), e38795.
23 P. Brandão, C. Marques, A. J. Burke and M. Pineiro, *Eur. J. Med. Chem.*, 2021, **5**(211), 113102.
24 C. Liang, J. Xia, D. Lei, X. Li, Q. Yao and J. Gao, *Eur. J. Med. Chem.*, 2014, **74**, 742–750.
25 Z. Ding, M. Zhou and C. Zeng, *Arch. Pharm.*, 2020, **353**, 1–13.

26 S. Kumar, S. T. Saha, L. Gu, G. Palma, S. Perumal, A. Singh-Pillay, P. Singh, A. Anand, M. Kaur and V. Kumar, *ACS Omega*, 2018, **3**, 12106–12113.
27 C. Wu, C. Du, J. Gubbens, Y. H. Choi and G. P. Van Wezel, *J. Nat. Prod.*, 2015, **78**, 2355–2363.
28 A. Medvedev, A. Kopylov, O. Buneeva, L. Kurbatov, O. Tikhonova, A. Ivanov and V. Zgoda, *Int. J. Mol. Sci.*, 2020, **21**, 1–23.
29 H. Guo, *Eur. J. Med. Chem.*, 2019, **164**, 678–688.
30 M. Solangi, Kanwal, K. M. Khan, S. Chigurupati, F. Saleem, U. Qureshi, Z. Ul-Haq, A. Jabeen, S. G. Felemban, F. Zafar, S. Perveen, M. Taha and S. Bhatia, *Arch. Pharm.*, 2022, **355**, 1–15.
31 H. M. Osman, T. Elsaman, B. A. Yousef, E. Elhadi, A. A. E. Ahmed, E. M. Eltayib, M. S. Mohamed and M. A. Mohamed, *J. Chem.*, 2012, **2021**, 1–11.
32 A. Mesripour, E. Jafari, M. R. Hajibeiki and F. Hassanzadeh, *Iran. J. Basic Med. Sci.*, 2023, **26**, 438–444.
33 S. M. Davis and T. J. Eckroat, *Med. Chem. Res.*, 2021, **30**, 2289–2300.
34 M. Valdés-Tovar, R. Estrada-Reyes, H. Solís-Chagoyán, J. Argueta, A. M. Dorantes-Barrón, D. Quero-Chávez, R. Cruz-Garduño, M. G. Cercós, C. Trueta, J. Oikawa-Sala, M. L. Dubocovich and G. Benítez-King, *Br. J. Pharmacol.*, 2018, **175**, 3200–3208.
35 R. K. Upadhyay, K. K. Saini, N. Deswal, T. Singh, K. P. Tripathi, P. Kaushik, N. A. Shakil, A. C. Bharti and R. Kumar, *RSC Adv.*, 2022, **12**, 24412–24426.
36 V. K. R. Tangadanchu, Y. F. Sui and C. H. Zhou, *Bioorg. Med. Chem. Lett.*, 2021, **41**, 128030.
37 X. M. Chu, C. Wang, W. L. Wang, L. L. Liang, W. Liu, K. K. Gong and K. L. Sun, *Eur. J. Med. Chem.*, 2019, **166**, 206–223.
38 S. Zhang, Z. Xu, C. Gao, Q. C. Ren, L. Chang, Z. S. Lv and L. S. Feng, *Eur. J. Med. Chem.*, 2017, **138**, 501–513.
39 S. Sathish Kumar and H. P. Kavitha, *Mini-Rev. Org. Chem.*, 2013, **10**, 40–65.
40 G. I. Lepesheva, R. D. Ott, T. Y. Hargrove, Y. Y. Kleshchenko, I. Schuster, W. D. Nes, G. C. Hill, F. Villalta and M. R. Waterman, *Chem. Biol.*, 2007, **14**, 1283–1293.
41 Y. Wang, R. Ding, Z. Tai, H. Hou, F. Gao and X. Sun, *Arabian J. Chem.*, 2022, **15**, 103639.
42 H. Singh, J. V. Singh, M. K. Gupta, A. K. Saxena, S. Sharma, K. Nepali and P. M. S. Bedi, *Bioorg. Med. Chem. Lett.*, 2017, **27**, 3974–3979.
43 S. K. Kancharla, S. Birudaraju, A. Pal, L. Krishnakanth Reddy, E. R. Reddy, S. K. Vagolu, D. Sriram, K. B. Bonige and R. B. Korupolu, *New J. Chem.*, 2022, **46**, 2863–2874.
44 Z. Wang and H. Qin, *Chem. Commun.*, 2003, **2**, 2450–2451.
45 P. M. Chaudhary, S. R. Chavan, F. Shirazi, M. Razdan, P. Nimkar, S. P. Maybhate, A. P. Likhite, R. Gonnade, B. G. Hazara, M. V. Deshpande and S. R. Deshpande, *Bioorg. Med. Chem.*, 2009, **17**, 2433–2440.
46 A. Singh, K. Kaur, H. Kaur, P. Mohana, S. Arora, N. Bedi, R. Chadha and P. M. S. Bedi, *J. Mol. Struct.*, 2023, **1274**, 134456.
47 M. H. Shaikh, D. D. Subhedar, V. M. Khedkar, P. C. Jha, F. A. K. Khan, J. N. Sangshetti and B. B. Shingate, *Chin. Chem. Lett.*, 2016, **27**, 1058–1063.